Pre-activation Distributions Expose Backdoor Neurons

Runkai Zheng *
School of Data Science
The Chinese University of Hong Kong, Shenzhen
Shenzhen
rkteddy@outlook.com

Rongjun Tang *
School of Science and Engineering
The Chinese University of Hong Kong, Shenzhen
Shenzhen
rongjuntang@link.cuhk.edu.cn

Jianze Li, Li Liu †
Shenzhen Research Institute of Big Data
The Chinese University of Hong Kong, Shenzhen
Shenzhen
lijianze@gmail.com, liuli@cuhk.edu.cn

Abstract

Convolutional neural networks (CNN) can be manipulated to perform specific behaviors when encountering a particular trigger pattern without affecting the performance on normal samples, which is referred to as backdoor attack. The backdoor attack is usually achieved by injecting a small proportion of poisoned samples into the training set, through which the victim trains a model embedded with the designated backdoor. In this work, we demonstrate that backdoor neurons are exposed by their pre-activation distributions, where populations from benign data and poisoned data show significantly different moments. This property is shown to be attack-invariant and allows us to efficiently locate backdoor neurons. On this basis, we make several proper assumptions on the neuron activation distributions, and propose two backdoor neuron detection strategies based on (1) the differential entropy of the neurons, and (2) the *Kullback-Leibler* (KL) divergence between the benign sample distribution and a poisoned statistics based hypothetical distribution. Experimental results show that our proposed defense strategies are both efficient and effective against various backdoor attacks. Source code is available here.

1 Introduction

Convolutional neural networks (CNNs) have achieved tremendous success during the past few years in a wide range of areas. However, training a CNN from scratch involves a large amount of data and expensive computational costs, which is sometimes infeasible. A more practical strategy is to obtain pretrained models or utilize public datasets from a third party, which brings convenience but also raises severe security problems into the deployment of models. For example, a malicious third party may provide pretrained models embedded with a designated backdoor, such that the model will have

*Eual Contribution
†Corresponding Author

36th Conference on Neural Information Processing Systems (NeurIPS 2022).

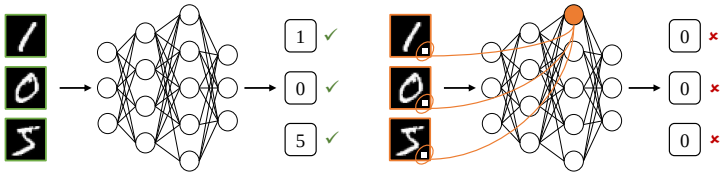

Figure 1: An overview of an infected learning system. The images with a white square are classified as class 0. It is an empirical observation that the backdoor behaviors are always triggered by one or more backdoor neurons.

a predefined response to some specific pattern, which is also called the *trigger*. More realistically, the attacker can inject only a small proportion of malicious data into the public dataset to mislead the trained model, which is referred to as *backdoor poisoning attacks* [26]. For instance, the malicious data can be created by patching a particular pattern into the benign data and changing the label to the desired target. The correlation between the trigger and the specified target label will be learned by the models during the training time. In this way, the infected model will misclassify the input to the attack target when the pattern is patched, while behaving normally otherwise, as shown in Figure 1.

Due to the limited understanding of CNNs, we are not clear on the formation mechanism of backdoor behaviors. However, it was empirically found that an infected model always possesses one or more neurons that have high correlation with the trigger activation, and pruning these neurons can significantly alleviate the backdoor behaviors, while retaining the model performance [43, 29, 7]. Nevertheless, how to precisely find out these backdoor neurons in an infected model is still a challenging problem, and has attracted a lot of attentions from the community.

In this work, we take an inspection on the pre-activation distributions of infected models on each layer. In general, the pre-activations in each neuron follow an unimodal distribution that can be approximated by a Gaussian distribution. However, we demonstrate that backdoor neurons do not hold such property. Instead, in a backdoor neuron, the pre-activation distributions of benign data and poisoned data present significant different moments, and can be approximated by a mixture of two Gaussian distributions. This property allows us to locate potential backdoor neurons through simple statistical analysis. Specifically, in case the defender has access to the poisoned dataset, the abnormal pre-activation distributions can be directly observed by forward propagating the data. The mixture of benign and poisoned data, where the small proportion of poisoned points being away from the benign mean, leads to a skewed, and even a bimodal distribution. Based on the maximum entropy property of the Gaussian distribution, the skewness will cause a reduction on the differential entropy, compared with a single Gaussian distribution with the same variance. Hence, after standardizing the pre-activation distribution to be unit variance, the abnormal distributions should have lower entropy. Those neurons could potentially separate benign and poisoned data. However, under the defense setting in which only an infected model and a small set of benign data are provided, we are not able to observe the bimodal distributions since the poisoned data is absent. In this case, we propose to rely on the statistics of *Batch Normalization* (BN) layers. Specifically, if the infected model is trained on poisoned data, the population statistics in backdoor neurons recorded in the BN layer will be different from that of only benign data. More importantly, the mismatch of statistics doesn't exist in benign neurons, making it possible to distinguish backdoor neurons. Based on the neuron entropy and the statistics discrepancy, we are able to locate and prune potential backdoor neurons to recover the model flexibly under two defense settings.

In summary, our contributions include:

1. We take a deep inspection on the infected model, and summarize the law of pre-activation distributions on poisoned dataset. We find that (1) the standardized entropy of backdoor neurons can be significantly lower than benign neurons, and (2) the BN statistics in infected model are mismatched with the benign sample statistics.

2. We propose to prune potential backdoor neurons based on either the differential entropy of pre-activation distribution or the statistics discrepancy, depending on the defense settings. Under certain assumptions, we claim that both the proposed indices can successfully separate the benign neurons and backdoor neurons by an appropriate threshold.

3. We conduct extensive experiments to verify our assumptions and evaluate our proposed methods, and achieve the state-of-the-art results under two different defense settings.

2 Related Work

In this section, we briefly discuss recent works in backdoor attack and defense, and a specific branch of related studies on distributional properties of poisoned features.

2.1 Backdoor attacks

The most famous *backdoor attack* is introduced in [15], where the adversary injects a small set of targeted label-flipped data with a specific trigger into the training set, leading to a misclassification when predicting the samples with such trigger. To make the trigger pattern even more invisible to human beings, the blending strategy is used in [6] to generate poison images, while the form of natural reflection is utilized in trigger design in [32]. The input image is perturbed in [41] to keep its content consistent with the target label such that the model better memorizes the trigger pattern, and keep it imperceptible to human beings. Moreover, the multi-target and multi-trigger attacks are proposed in [45, 34], and make the attack more flexible and covert. Recently, some sample-specific trigger design strategies [28] are proposed, making the defense against such backdoor attack much harder. Generally, the above attacks can be referred to as the *poisoning based backdoor attacks*.

Under some settings, the attackers can control the training process to inject the backdoor without modifying the training data, referred as the *non-poisoning based backdoor attacks*. This is achieved in [31, 37, 5] through targeted modification of the neurons' weight in a network. Such attacks will not be evaluated in our work due to its strong attack setting.

2.2 Backdoor defenses

Training stage defense. Under such setting, the defender has access to the training process, so that they can detect and filter the poisoned data or add some restrictions to suppress the backdoor effect in training. Since the poisoned data can be regarded as outliers, different strategies are applied in [10, 13, 1, 40, 16], such as the *robust statistics* in feature space and *input perturbation techniques* to filter them out of training data. Other methods aim at suppressing the backdoor effect during training phase with strong data augmentation methods [2] [27] [36] [33] including *CutMix* [46], *Flip*, *ShrinkPad* [27], *CutOut* and *MaxUp* [14], or *differential privacy* constraints [12, 19].

Model post-processing defense. Under some specific scenarios, the defenders are only given a suspicious DNN model without access to the training process or the full training set. Therefore, they must eliminate the backdoor threat with limited resources, such as a small set of clean data. A straightforward way is to reconstruct the trigger, and then mitigate the model with the knowledge of the reversed trigger [42]. Some try to find the relationship between backdoor behaviors and the neurons in a DNN model. Different levels of stimulation to a neuron are introduced in [30] to see how to determine the output activation change, if the model is attacked. Simple neuron pruning strategies are applied in [7] to repair the model, while redundant neuron pruning and fine-tuning are combined in [29] to erase the backdoor effect. Adversarial perturbations are added to the neurons in [43] and precisely prunes the easily-perturbed neurons with more limited clean data requirement and better performance. There are other fine-tuning based methods with the implementation of knowledge distillation [25, 18]. Mode connectivity repair technique [47] is also explored to mitigate the backdoored model. Recently, the *K-Arm optimization* [39] is applied in backdoor detection, helping curtail the threat of backdoor attack.

2.3 Distributional properties in poisoned dataset

Especially, one branch of backdoor learning studies the distributional properties of benign and poisoned samples. To be specific, they seek for filtering out malicious data utilizing the statistical differences of poisoned samples. Activation clustering [4] use K-means to separate benign and poisoned samples in feature space. Spectral signatures [40] reveal that feature vectors tend to leave strong signals in the top eigenvectors of their covariance matrix. SPECTRE (Spectral Poison Excision Through Robust Estimation)[7] utilizes tools from robust statistics to amplify the spectral signature

by outlier-robust data whitening. Our work differentiated from the above works from the following three aspects: 1) the above works focus on the penultimate layer feature representation, while our work inspects deep into each layer 2) the above works take the representation space from all neurons as a whole, while our finding indicates that the distributional difference only exists in some neurons 3) the above works aim at filtering out poisoned samples for retraining, while our methods directly repair the trained neural network by pruning potential backdoor neurons.

3 Preliminaries

3.1 Notations

Consider a multi-class classification problem with C classes. Let the original training set $\mathcal{D} = \{(\boldsymbol{x}_i, y_i)\}_{i=1}^N$ contains N i.i.d. sample images $\boldsymbol{x}_i \in \mathbb{R}^{d_c \times d_h \times d_w}$ and the corresponding labels $y_i \in \{1, 2, ..., C\}$ drawn from $\mathcal{X} \times \mathcal{Y}$. Here, we denote by d_c, d_h and d_w the number of neurons, the height and the width of images, respectively. In particular, we have $d_c = 3$ for RGB images.

As in Section 2.1, the backdoor poisoning attack involves changes to the input images and the corresponding labels on a subset $\mathcal{D}_p \subseteq \mathcal{D}$. In this work, we define the ratio $\rho = \frac{|\mathcal{D}_p|}{|\mathcal{D}|}$ as the *poisoning rate*. We denote the poisoning function to the input images as $\delta(\boldsymbol{x})$. A dataset $\mathcal{D}$ is said to be ρ-poisoned if the poisoning rate of the dataset is ρ.

Consider a neural network $F(x; \theta)$ with L layers. Denote

$$F^{(l)} = f^{(l)} \circ \phi \circ f^{(l-1)} \circ \phi \circ \cdots \circ \phi \circ f^{(1)},$$

for $1 \leq l \leq L$, where $f^{(l)}$ is a linear function (*e.g.*, convolution) in the l-th layer, and ϕ is a nonlinear activation function applied element wise. In this work, we may denote $F(x; \theta)$ as $F(x)$ or F for simplicity.

We denote by $\boldsymbol{W}^{(l)} \in \mathbb{R}^{d_{c'} \times d_c \times d_h \times d_w}$ the weight tensor of a convolutional layer. To do pruning, we apply a mask $\boldsymbol{M}^{(l)} \in \{0, 1\}^{d_{c'} \times d_c \times d_h \times d_w}$ starting with $\boldsymbol{M}^{(l)} = \mathbb{1}_{d_{c'} \times d_c \times d_h \times d_w}$ in each layer. Pruning neurons on the network refers to getting a collection of indices $\mathcal{I} = \{(l, k)_i\}_{i=1}^I$ and setting $\boldsymbol{M}_k^{(l)} = \mathbf{0}_{d_c \times d_h \times d_w}$ if $(l, k) \in \mathcal{I}$. The pruned network $F_{-\mathcal{I}}$ has the same architecture as F but with all the weight matrices of convolutional layers set to $\boldsymbol{W}^{(l)} \odot \boldsymbol{M}^{(l)}$, where $\odot$ denotes the Hadamard product.

3.2 Differential entropy

To measure the uncertainty of a discrete random variable Z, the *entropy* [38, 8] was defined as $H(Z) = -\sum_{z \in Z} p(z) \log p(z)$. At the same time, as an extension of entropy, the *differential entropy* was also introduced for a continuous random variable. More concretely, if Z is a continuous random variable, then it was defined as

$$h(Z) = -\int_Z p(z) \log p(z) dz. \tag{1}$$

An important fact about the differential entropy is that, among all the real-valued distributions supported on $(-\infty, \infty)$ with a specified finite variance, the Gaussian distribution maximizes the differential entropy [8]. In this work, the differential entropy (1) will be utilized to identify the distributions that are far different from a Gaussian distribution.

3.3 Backdoor neurons

It was found that there exist one or more neurons that contribute the most to the backdoor behaviors in a infected model [43, 29]. If some of or all of these neurons are pruned, the *attack success rate* will be reduced greatly [43]. In this work, to better quantify the importance of neurons to backdoor behaviors, we would like to introduce the sensitivity of neurons to the backdoor. We first introduce the definition of *backdoor loss* on a specific poisoning function:

Definition 1. Given a model F and a poisoning function δ, the backdoor loss on the dataset $\mathcal{D}$ is defined as:

$$\mathcal{L}_{\mathrm{bd}}(f) = \mathbb{E}_{(\boldsymbol{x}, y) \sim \mathcal{D}}[\mathrm{D}_{\mathrm{CE}}(y, f(\delta(\boldsymbol{x}))],$$

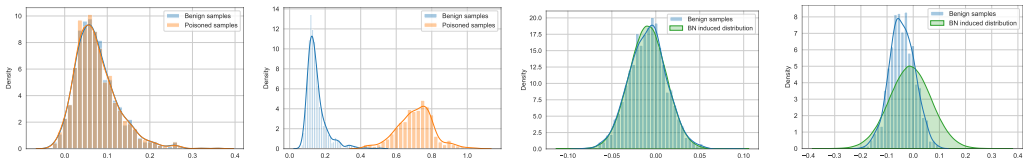

(a) Benign neuron (b) Backdoor neuron (c) Benign neuron (d) Backdoor neuron

Figure 2: In (a) and (b), we compare the pre-activation distributions in backdoor neurons and benign neurons. In benign neurons, the pre-activation distributions on benign data and poisoned data are nearly the same, while in backdoor neurons, they show a great difference. In (c) and (d), we plot the empirical distributions with benign samples (in blue) and the BN statistics induced Gaussians (in green). In backdoor neurons, the discrepancy between the empirical and BN-induced distribution is large (all the neurons are selected from infected ResNet-18 trained on CIFAR-10, and use 1,000 images with (poisoned data) or without trigger (benign data) as the inputs).

where D_{CE} denotes the cross entropy loss.

Then:

Definition 2. Given a model F, the index of a neuron (l, k) and the backdoor loss $\mathcal{L}_{\mathrm{bd}}$, the sensitivity of that neuron to the backdoor is defined as:

$$\alpha(F, l, k) = \mathcal{L}_{\mathrm{bd}}(F) - \mathcal{L}_{\mathrm{bd}}(F_{-\{(l,k)\}}), \tag{2}$$

where $F_{-\{(l,k)\}}$ is the network after pruning the k-th neuron of the l-th layer.

The backdoor loss is high when the model is infected, and will be reduced when the backdoor effect is alleviated.

Using the quantity defined in (2), we are now able to find the neurons that are mostly correlated with the backdoor behaviors:

Definition 3. Given a model F and a threshold $\tau > 0$, the set of backdoor neurons are defined as:

$$\mathcal{B}_{F,\tau} = \{(l, k) : \alpha(F, l, k) > \tau\}. \tag{3}$$

3.4 Pre-activation distribution

During the forward propagation of an input $\boldsymbol{x}$, we denote $\boldsymbol{x}^{(l)} = F^{(l)}(\boldsymbol{x}) \in \mathbb{R}^{d_c^{(l)} \times d_h^{(l)} \times d_w^{(l)}}$ as the output of the l-th layer. For the k-th neuron of the l-th layer, the *pre-activation* $\boldsymbol{\phi}_k^{(l)} = \phi(\boldsymbol{x}_k^{(l)})$ is defined as the maximum value of the k-th slice matrix of dimension $d_h^{(l)} \times d_w^{(l)}$ in $\boldsymbol{x}^{(l)}$. The reason we choose *pre-activations* instead of *activations* is that the distribution of activations after non-linear function might be distorted. For example, ReLU (rectified linear unit) will cut out all negative values.

It is a common assumption that, for every neuron, the pre-activations before the non-linear function follow a Gaussian distribution, if the network is randomly initialized and the number of neurons is large enough [22]. This assumption is based on the central limit theorem under weak dependence [3]. In a trained network, although this assumption may not strictly hold, the pre-activation of every neuron can be still regarded as approximately following a Gaussian distribution. However, in this work, for the first time, we observe a bimodal pre-activation distribution in backdoor neurons formed by the benign data and poisoned data. This phenomenon is shown in Figure 2, where a typical backdoor neuron is compared with the benign neurons. It can be seen that, after the model is infected, the pre-activation distributions of benign neurons hardly change when the data is poisoned, while the pre-activation distributions of backdoor neurons become significantly different.

4 Methodology

4.1 Basic Assumptions

We now introduce two preliminarily assumptions on the pre-activation distribution of an infected neural network.

Assumption 1. Given an infected model F, we have $|\mathcal{B}_{F,\tau}| > 0$ for some threshold $\tau > 0$.

This is a primary assumption that guarantees proper pruning of neurons can correct the network's predictions on poisoned samples to some extent. Hence, it is a prerequisite of good performance of all the pruning-based defense methods.

The next assumption provides a precondition for our methods.

Assumption 2. Given a model F infected by a poisoning function δ with a ρ-poisoned dataset $\mathcal{D}$, the pre-activation of sample from $\mathcal{D}$ on each single neuron of F follow a Gaussian mixture distribution, that is:

$$\boldsymbol{\phi}_k^{(l)} \sim (1-\rho)\mathcal{N}(\mu_k^{(l)}, \sigma_k^{(l)2}) + \rho\mathcal{N}(\hat{\mu}_k^{(l)}, \hat{\sigma}_k^{(l)2}),$$

with

$$|\mu_k^{(l)} - \hat{\mu}_k^{(l)}| \begin{cases} < \epsilon, & \text{if } (l,k) \notin \mathcal{B}_{F,\tau}, \\ \gg \epsilon, & \text{if } (l,k) \in \mathcal{B}_{F,\tau}, \end{cases}$$

and

$$|\sigma_k^{(l)2} - \hat{\sigma}_k^{(l)2}| < \epsilon, \quad \forall k \notin \mathcal{B}_{F,\tau}$$

where $\epsilon > 0$ is a small enough value, $\mu_k^{(l)}$ and $\sigma_k^{(l)2}$, $\hat{\mu}_k^{(l)}$ and $\hat{\sigma}_k^{(l)2}$ are the mean and variance of $\{\phi(F^{(l)}(\boldsymbol{x})_k) : \boldsymbol{x} \sim \mathcal{X}\}$, $\{\phi(F^{(l)}(\delta(\boldsymbol{x}))_k) : \boldsymbol{x} \sim \mathcal{X}\}$, respectively.

This assumes that the mean value of pre-activation distribution of benign and poisoned samples only significantly differentiated in backdoor neurons. This assumption is made based on empirical observation, and our methods work only when this assumption holds.

4.2 Entropy-based Pruning (EP)

If the pre-activation distributions are standardized (subtracting the mean and dividing the standard deviation), the differential entropy will be maximized on the benign neuron approximately following a standard Gaussian distribution $\mathcal{N}(0,1)$. In backdoor neurons, because of the difference of the moments on Gaussian components, the resulting mixture distributions can not be Gaussian distributions, hence the differential entropy must be smaller than that of a standardized Gaussian distribution.

Corollary 1. Let $\dot{\boldsymbol{\phi}}_k^{(l)} = \frac{\boldsymbol{\phi}_k^{(l)} - \mu_k^{(l)}}{\sigma_k^{(l)}}$ be the standardized pre-activations, then the following inequality is satisfied:

$$h(\dot{\boldsymbol{\phi}}_k^{(l)}) < h(\dot{\boldsymbol{\phi}}_{k'}^{(l)}) \leq h(Z), \quad \forall k \in \mathcal{B}_{F,\tau}, k' \notin \mathcal{B}_{F,\tau},$$

where $Z \sim \mathcal{N}(0,1)$ is the standardized Gaussian distribution.

This inequality gives a guarantee that with an appropriately chosen threshold, the backdoor neurons can be well separated with the benign neurons.

4.3 BN statistics-based Pruning (BNP)

BN layer involves using the statistics of a mini-batch to normalize the data in each layer for each neuron. It is known to be able to smooth the optimization landscape, and has gradually become a default setting of neural networks [20]. When inference, BN uses the fixed statistics obtained by averaging the sample statistics of mini-batches during training time, including the mean and the variance. If the model is trained on a poisoned dataset, BN will record the mean and the variance of the poison-benign mixed data. Note that the mean and variance here are not defined on the pre-activations $\boldsymbol{\phi}_k^{(l)}$, but on $\boldsymbol{x}_k^{(l)}$. Based on the above discussions, we know that the poisoned pre-activations in backdoor neurons follow a different distribution from the benign samples. The recorded statistics during training are actually that of the mixture distribution. Hence, we can expect that the BN statistics of a trained backdoor neural network are biased. If we are able to access a small set of benign data, we can calculate an approximation of the true statistics on benign data. Then we calculate the *Kullback-Leibler* (KL) divergence [9] between the sample distribution and the BN induced distribution as the measurement of the bias. By assuming both of the distributions follow Gaussian distributions, we have a closed-form solution:

$$\mathrm{D}_{\mathrm{KL}}(\mathcal{N}_{\text{sample}}^{(l)}, \mathcal{N}_{\text{BN}}^{(l)})_k = \log \frac{\tilde{\sigma}_k^{(l)}}{\sigma_k^{(l)}} + \frac{\sigma_k^{(l)2} + (\mu_k^{(l)} - \tilde{\mu}_k^{(l)})^2}{2\tilde{\sigma}_k^{(l)2}} - \frac{1}{2},$$

where $\mathcal{N}_{\text{sample}}^{(l)} = \mathcal{N}(\mu_k^{(l)}, \sigma_k^{(l)2})$, $\mathcal{N}_{\text{BN}}^{(l)} = \mathcal{N}(\tilde{\mu}_k^{(l)}, \tilde{\sigma}_k^{(l)2})$, $\mu_k^{(l)}$ and $\sigma_k^{(l)2}$ are the statistics obtained from benign samples, $\tilde{\mu}_k^{(l)2}$ and $\tilde{\sigma}_k^{(l)}$ are the BN statistics. Note that BN statistics is the mixture statistics of benign and poisoned distributions. Thus, we have the following corollary:

Corollary 2. According to Assumption 2, when $\epsilon \to 0$, the following inequality is satisfied:

$$\mathrm{D_{KL}}(\mathcal{N}_{\text{sample}}^{(l)}, \mathcal{N}_{\text{BN}}^{(l)})_k > \mathrm{D_{KL}}(\mathcal{N}_{\text{sample}}^{(l)}, \mathcal{N}_{\text{BN}}^{(l)})_{k'} = 0, \quad \forall k \in \mathcal{B}_{F,\tau}, k' \notin \mathcal{B}_{F,\tau},$$

The corollary indicates that backdoor neurons should have larger KL divergences than benign neurons, as illustrated in Figure 2(c).

4.4 Overview of the two pruning strategies

In Section 3.4, we reveal the discrepancy between the pre-activation distributions in backdoor neurons and that in the benign neurons. This enables fast detecting the neurons that are more related to the backdoor behaviours. The index we choose to detect the abnormal neurons depends on what kind of data we are able to access.

Mixture training data In this case, the victim is given a poisoned training dataset with a specified poisoning rate ρ. Our goal is to obtain a benign model based on the poisoned dataset. To achieve this, we first train an infected model F on the poisoned dataset. The resulting model should have a certain number of backdoor neurons based on empirical observation and assumption. Since $\rho > 0$ for the dataset, all the neurons follow Gaussian mixture distributions, and we have $h(\dot{\boldsymbol{x}}_k^{(l)}) < h(\dot{\boldsymbol{x}}_{k'}^{(l)})$ for all $k \in \mathcal{B}_{F,\tau}, k' \notin \mathcal{B}_{F,\tau}$. This implies that with an appropriate threshold τ_h^*, we can perfectly separate the benign neurons and backdoor neurons, which can be formulated as:

$$\begin{aligned} \exists \tau_h^*, \quad & h(\dot{\boldsymbol{x}}_k^{(l)}) < \tau_h^*, \quad \forall k \in \mathcal{B}_{F,\tau}, \\ & h(\dot{\boldsymbol{x}}_{k'}^{(l)}) > \tau_h^*, \quad \forall k' \notin \mathcal{B}_{F,\tau}. \end{aligned}$$

Setting the threshold τ_h^* is crucial to the solution, and it is a trade-off between the accuracy on benign samples and that on the backdoored samples. Note that $|\mathcal{B}_{F,\tau}^{(l)}| << d_c^{(l)}$. We can treat the low entropy neurons as outliers in each layer, and set different thresholds for different layers. Specifically, let $h^{(l)} = [h(x_1^{(l)}), h(x_2^{(l)}), \ldots, h(x_{d_c^{(l)}}^{(l)})]^T \in \mathbb{R}^{d_c^{(l)}}$ be a vector of differential entropy of the l-th layer calculated from the poisoned dataset. Then we set $\tau_h^{(l)} = \bar{h}^{(l)} - u_h \cdot s_h^{(l)}$, where $\bar{h}^{(l)} = \frac{1}{d_c^{(l)}} \sum_{k=1}^{d_c^{(l)}} h_k^{(l)}$ and $s_h^{(l)} = \sqrt{\frac{1}{d_c^{(l)}} \sum_{k=1}^{d_c^{(l)}} (h_k^{(l)} - \bar{h}^{(l)})^2}$ are the mean and standard deviation of $h^{(l)}$, u_h is a hyperparameter controlling how low the threshold is. Then we have a set of indices of potential backdoor neurons $\mathcal{I}_h = \{(l,k) : h_k^{(l)} < \tau_h^{(l)}\}$. Finally, we prune the infected model F using $\mathcal{I}_h$, which results in a final model $F_{-\mathcal{I}_h}$.

Benign training data This is the case that the victim is given a trained poisoned model F with a small set of benign data. Our goal is to utilize the benign data to clean up the poisoned model and eliminate the backdoor threat. Similar to the pruning process based on differential entropy, we first construct a vector of KL divergences of all neurons for each layer $K^{(l)} = [K_1^{(l)}, K_2^{(l)}, \ldots, K_{d_c^{(l)}}^{(l)}]^T \in \mathbb{R}^{d_c^{(l)}}$ according to equation (4). We set $\tau_K^{(l)} = \bar{K}^{(l)} - u_K \cdot s_K^{(l)}$, where $\bar{K}^{(l)} = \frac{1}{d_c^{(l)}} \sum_{k=1}^{d_c^{(l)}} K_k^{(l)}$ and $s_K^{(l)} = \sqrt{\frac{1}{d_c^{(l)}} \sum_{k=1}^{d_c^{(l)}} (K_k^{(l)} - \bar{K}^{(l)})^2}$ are the mean and standard deviation of $K^{(l)}$, u_K is a hyperparameter. The set of selected neurons is $\mathcal{I}_K = \{(l,k) : K_k^{(l)} < \tau_K^{(l)}\}$ and the pruned model can be represented as $F_{-\mathcal{I}_K}$.

5 Experiments

5.1 Implementation details

Datasets In this section, the experiments are conducted on two influential benchmarks, CIFAR-10 [23] and Tiny-ImageNet [24]. We use 90% of the data set for training, the rest of the data is used for validating or recovering the poisoned model.

Models We use ResNet-18 [17] as the baseline model to evaluate our proposed method, and compare it with other methods. We train the network for 150 epochs on CIFAR-10 and 100 epochs on Tiny-ImageNet with SGD optimizer. The initial learning rate is set to 0.1 and the momentum is set to 0.9. We adopt the cosine learning rate scheduler to adjust the learning rate. The batch size is set to 128 by default.

Attacks Our experiments are based on both the classical and the most advanced attack strategies, including the *BadNet* [15], *Clean Label Attack* (CLA) [41], *Reflection Backdoor* (Refool) [32], *Warping-based poisoned Networks* [35], *Blended backdoor attack* (Blended) [6], *Input-aware backdoor attack* (IAB) [34] and *Sample Specific Backdoor Attack* (SSBA) [28]. For BadNets, we test both the *All-to-All* (A2A) attack and *All-to-One* (A2O) attack, *i.e.*, the attack target labels are set to $y_t = (y + 1) \bmod C$, or one particular label $y_t = C_t$, respectively. The target for A2O attacks of all the attack strategies is set to class 0. The triggers for BadNets and CLA are set to randomly generated patterns with size 3×3 for CIFAR-10 and 5×5 for Tiny-ImageNet. The poisoning rate is set to 10% by default. Note that, due to the image size restraint, SSBA is only performed on Tiny-Imagenet.

Defenses We conduct experiments under two defense settings, one of which allows the defender to access the poisoned training set, while the other only has a small clean data set. Both the defense goals are to obtain a clean model without backdoor behaviours. We compare our approaches with the l_∞ *pruning* [7], *fine-tuning* (FT), *fine-pruning* (FP) [29] and *neural attentional distillation* (NAD) [25]. The number of benign samples allowed to access is set to 500 (1%) for CIFAR-10 and 5000 (5%) for Tiny-ImageNet by default. We set the threshold hyperparameter u_h/u_k to 3 on CIFAR-10 and 4 on Tiny-ImageNet of all tested attacks by default.

Evaluation metrics In this work, we use the *attack clean accuracy* (ACC) and *attack success rate* (ASR) to evaluate the effectiveness of different methods. The ACC for a given model F is defined as:

$$\mathrm{ACC}(F, \mathcal{D}_{\mathrm{test}}) = \sum_{(\boldsymbol{x},y)\in\mathcal{D}_{\mathrm{test}}} \mathbb{I}\{\mathrm{argmax}(F(\boldsymbol{x})) = y\},$$

where $\mathbb{I}$ is the *indicator function*. The ASR is defined as:

$$\mathrm{ASR}(F, \mathcal{D}_{\mathrm{test}}) = \sum_{(\boldsymbol{x},y)\in\mathcal{D}_{\mathrm{test}}, y\neq y_t} \mathbb{I}\{\mathrm{argmax}(F(\delta(\boldsymbol{x}))) = y_t\},$$

where y_t is the attack target label. The ACC measures the model performance on benign samples, while the ASR reflects the degree of backdoor behavior retainment in the model. Given an infected model, our goal is to reduce the ASR, while keeping the ACC from dropping too much.

5.2 Experimental results

CIFAR-10 We show the results on CIFAR-10 in Table 1. The recently proposed NAD and ANP perform significantly better than other defense methods, reducing the ASR to a very low level with a slight drop on ACC. However, they also have a significant drop ($3 \sim 4\%$) on ACC when defending CLA, which is the most robust backdoor attack in our experiments, and ANP even failed when defending BadNets(A2A). Nevertheless, both of our methods successfully eliminate the backdoor (ASR $< 1\%$) with negligible loss on ACC. We even observe a little rise on ACC when defending BadNets by EP. This phenomenon demonstrates that backdoor neurons may hurt the ACC in some way, and thus the ACC will rise when the backdoor neurons are precisely pruned. Overall, our methods achieve the most advanced defense results.

Table 1: Experimental results of the proposed approaches against different attacks compared with other defense methods in CIFAR-10[23].

	BadNets (A2O)		BadNets (A2A)		CLA		WaNet		Blended		Refool		IAB	
Attacks	ACC	ASR	ACC	ASR	ACC	ASR	ACC	ASR	ACC	ASR	ACC	ASR	ACC	ASR
Origin	93.86	100.00	94.60	93.89	94.99	98.83	94.11	99.67	94.17	99.62	94.24	98.40	93.87	97.91
FT	92.22	2.16	92.03	60.76	92.88	95.73	92.93	9.37	93.9	90.27	91.68	17.78	91.78	9.52
FP	92.18	2.97	91.75	66.82	92.60	99.36	92.07	1.03	70.92	90.92	92.36	75.98	87.04	16.13
l_∞	92.12	100.00	93.67	6.67	92.75	98.76	93.48	99.74	86.99	99.77	91.19	98.47	88.37	88.48
NAD	93.36	2.43	92.18	2.06	91.36	15.31	93.08	3.05	92.72	1.61	91.64	6.74	92.11	19.45
ANP	93.47	3.53	90.29	86.22	91.13	11.76	**94.12**	**0.51**	93.66	5.03	91.71	26.96	**93.52**	10.61
EP (Ours)	**93.88**	**0.86**	**94.49**	**0.61**	**94.42**	**0.91**	93.79	2.80	93.67	**2.24**	93.35	8.90	93.17	0.94
BNP (Ours)	93.60	1.60	94.25	0.72	94.14	7.03	94.05	3.39	**94.17**	2.71	**93.69**	**6.48**	93.15	**0.64**

Table 2: Experimental results of the proposed approaches against different attacks compared with other defense methods in Tiny-ImageNet[24].

	BadNets (A2O)		CLA		WaNet		Refool		Blended		IAB		SSBA	
Attacks	ACC	ASR	ACC	ASR	ACC	ASR	ACC	ASR	ACC	ASR	ACC	ASR	ACC	ASR
Origin	61.36	97.38	65.61	56.58	61.47	99.98	53.26	80.61	62.85	99.83	61.40	98.28	66.51	99.78
FT	46.93	99.84	61.19	63.20	54.28	99.96	47.09	91.77	56.83	29.12	52.39	99.1	52.39	33.19
FP	35.41	99.48	62.30	39.05	53.65	100.00	42.10	86.62	59.59	99.76	52.67	98.47	53.36	31.96
l_∞	53.13	90.39	59.15	23.12	42.01	99.84	46.84	81.19	56.33	99.85	54.81	86.97	49.35	99.98
NAD	44.20	90.13	62.80	17.35	53.40	99.98	51.06	70.63	57.35	55.6	53.32	98.85	52.52	25.08
ANP	53.85	4.02	59.69	3.64	54.82	86.98	50.67	**0.21**	**62.49**	**0.61**	**61.39**	4.67	60.98	1.01
EP (Ours)	60.68	**0.86**	64.47	0.10	60.53	0.02	51.29	17.07	60.67	**0.69**	61.26	**0.60**	64.2	0.11
BNP (Ours)	**61.60**	1.60	**64.86**	**0.05**	**61.58**	**0.01**	**52.41**	23.79	60.77	0.85	**61.30**	**0.60**	**64.64**	**0.01**

Tiny-ImageNet Tiny-ImageNet is a larger scale dataset with higher resolution images, and it is harder to defend against the attacks performed on it. Note that the A2A attack is absent, since we cannot successfully perform the attack due to the large number of its classes (up to 200). Our experimental results show that all the defense methods suffer from the performance degradation compared with the results in CIFAR-10, and they fail to defend against WaNet with a large ACC drop but even unchanged ASR, especially the ANP and l_∞ defense. This phenomenon shows that the principles for finding backdoor neurons of both ANP and l_∞ don't work in such case. Nevertheless, our methods totally remove the backdoor and the ACC are not even affected, which indicates that our methods can precisely locate the backdoor neurons even on such large scale dataset.

5.3 Ablation study

To be fair, we compare BNP with other re-training based methods using 500 benign samples in Section 5.2. However, BNP doesn't require re-training the model, and the samples are just used for detecting the distribution discrepancy. As the statistical differences may be detected with much fewer samples, we now study how the number of samples affects the effectiveness of BNP. We train BadNets, CLA, Refool and Blended on CIFAR-10 with $\rho = 10\%$, and use 10 to 500 benign samples to recover the model using BNP. We record the changes of ACC and ASR with respect to the number of benign samples. The results are shown in Section 5.3. The influence of the number of samples to our methods comes from the randomness on estimating moments. As the number of samples grows, the randomness is reduced and BNP has more stable performance, but the average performances are not improved, except for Refool. Compared with other attacks, Refool clearly needs more samples to reduce the ASR. A possible reason is that the mixture distribution in Refool has closer moments and is harder to distinguish. Besides, we surprisingly find that BNP can recover BadNets, CLA and Blended using only 10 benign samples. We also conduct experiments to show the high correlation between the backdoor neurons and our proposed evaluation metrics, the results are shown in Appendix D.

6 Discussion

The proposed methods are superior to other existing defense methods in the following three aspects:

Better performance As demonstrated in Section 5, both of the proposed methods achieve state-of-the-art results. Moreover, according to the ablation study, the proposed BNP can successfully defend most of the attacks within 10 benign samples, which shows the amazing effectiveness of our proposed methods.

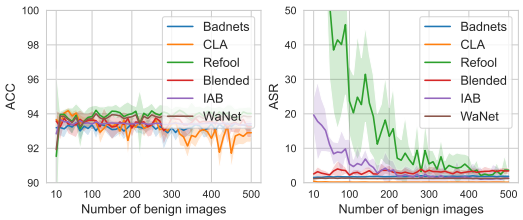

Figure 3: This figure shows the influence of samples used for BNP.

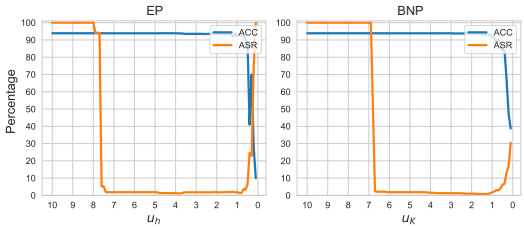

Figure 4: This figure shows the performance of the proposed EP and BNP with different hyperparameter against badnet on CIFAR-10 with ResNet-18.

Higher efficiency The proposed methods are also highly efficient. We record the running time of several defense methods on 500 CIFAR-10 images with ResNet-18, and show the results in Table 3. It can be seen that both of the proposed methods require less time than the baseline defense methods. Since both methods require scanning on each neuron once, the computational complexity scale linearly with the number of the neurons in the neural network. Therefore, the efficiency of our methods is promised.

Table 3: The overall running time of different defense methods on 500 CIFAR-10 images with ResNet-18.

Defense Method	FT	FP	NAD	ANP	EP (ours)	BNP (ours)
Runing Time (sec.)	12.35s	$14.59s$	$22.08s$	$25.68s$	$10.69s$	**0.39s**

More robust to hyperparameter choosing One of the most general problems in backdoor defense is the choice of hyperparameters. Under realistic settings, the defenders can only perform defenses without any prior knowledge about poison data, including poisoning rate and examples of poisoned data. So the defenders should carefully tune the hyperparameters, or the ACC and ASR can change suddenly even under small fluctuations of those hyperparameters. In comparison, both of the proposed pruning strategies only require one universal hyperparameter u. Moreover, they show reliable consistency against different attacks in the same dataset, only vary from different datasets, which is inevitable. Besides, we leave a wide range of parameters to choose, so that the ACC remains high while the ASR is controlled to a very small number, as shown in Section 5.3.

7 Conclusion

In this work, we take a deep inspection on the pre-activation distributions in each layer, and study their characteristics in an infected model. We find that the distributions of benign data and poisoned data on these neurons are both Gaussian, but extraordinarily different in their moments. The mixture distributions have low entropy compared with that of the benign neurons. This property makes it possible for the defender to efficiently detect the abnormal neurons based on the sample entropy, when the poisoned dataset can be accessed. Moreover, when the defender has only a small set of benign data, we propose to detect the abnormal neurons based on the inconsistency of the BN statistics on poisoned dataset and the sample statistics on the given benign dataset. We then do pruning on these potential backdoor neurons using the proposed two detection methods to recover the model. The experiments show that the proposed defending strategies can efficiently locate the backdoor neurons, and greatly reduce the backdoor threat with negligible loss on clean accuracy. Our approach based on the pre-activation distributions achieves superior results compared with all other defense methods under various attacks on both datasets, empirically showing that the distribution property may be both dataset-invariant and attack-invariant. The results shed lights on the field of backdoor defense, and can be a guidance for designing more robust backdoor attacks.

References

[1] Hassan Ali, Surya Nepal, Salil S Kanhere, and Sanjay Jha. Has-nets: A heal and select mechanism to defend dnns against backdoor attacks for data collection scenarios. *arXiv preprint arXiv:2012.07474*, 2020.

[2] Eitan Borgnia, Valeriia Cherepanova, Liam Fowl, Amin Ghiasi, Jonas Geiping, Micah Goldblum, Tom Goldstein, and Arjun Gupta. Strong data augmentation sanitizes poisoning and backdoor attacks without an accuracy tradeoff. In *ICASSP 2021-2021 IEEE International Conference on Acoustics, Speech and Signal Processing (ICASSP)*, pages 3855–3859. IEEE, 2021.

[3] Richard C Bradley Jr. Central limit theorems under weak dependence. *Journal of Multivariate Analysis*, 11(1):1–16, 1981.

[4] Bryant Chen, Wilka Carvalho, Nathalie Baracaldo, Heiko Ludwig, Benjamin Edwards, Taesung Lee, Ian Molloy, and Biplav Srivastava. Detecting backdoor attacks on deep neural networks by activation clustering. *arXiv preprint arXiv:1811.03728*, 2018.

[5] Huili Chen, Cheng Fu, Jishen Zhao, and Farinaz Koushanfar. Proflip: Targeted trojan attack with progressive bit flips. In *Proceedings of the IEEE/CVF International Conference on Computer Vision*, pages 7718–7727, 2021.

[6] Xinyun Chen, Chang Liu, Bo Li, Kimberly Lu, and Dawn Song. Targeted backdoor attacks on deep learning systems using data poisoning. *arXiv preprint arXiv:1712.05526*, 2017.

[7] Hao Cheng, Kaidi Xu, Sijia Liu, Pin-Yu Chen, Pu Zhao, and Xue Lin. Defending against backdoor attack on deep neural networks. *CoRR*, abs/2002.12162, 2020.

[8] Thomas M. Cover and Joy A. Thomas. *Elements of Information Theory*. John Wiley & Sons, 2012.

[9] Imre Csiszár. I-divergence geometry of probability distributions and minimization problems. *The annals of probability*, pages 146–158, 1975.

[10] Bao Gia Doan, Ehsan Abbasnejad, and Damith C. Ranasinghe. Februus: Input purification defense against trojan attacks on deep neural network systems. In *Annual Computer Security Applications Conference*, ACSAC '20, page 897–912, New York, NY, USA, 2020. Association for Computing Machinery.

[11] Khoa Doan, Yingjie Lao, and Ping Li. Backdoor attack with imperceptible input and latent modification. In A. Beygelzimer, Y. Dauphin, P. Liang, and J. Wortman Vaughan, editors, *Advances in Neural Information Processing Systems*, 2021.

[12] Min Du, Ruoxi Jia, and Dawn Song. Robust anomaly detection and backdoor attack detection via differential privacy. In *International Conference on Learning Representations*, 2019.

[13] Yansong Gao, Change Xu, Derui Wang, Shiping Chen, Damith C Ranasinghe, and Surya Nepal. Strip: A defence against trojan attacks on deep neural networks. In *Proceedings of the 35th Annual Computer Security Applications Conference*, pages 113–125, 2019.

[14] Chengyue Gong, Tongzheng Ren, Mao Ye, and Qiang Liu. Maxup: A simple way to improve generalization of neural network training. *arXiv preprint arXiv:2002.09024*, 2020.

[15] Tianyu Gu, Kang Liu, Brendan Dolan-Gavitt, and Siddharth Garg. Badnets: Evaluating backdooring attacks on deep neural networks. *IEEE Access*, 7:47230–47244, 2019.

[16] Jonathan Hayase and Weihao Kong. Spectre: Defending against backdoor attacks using robust covariance estimation. In *International Conference on Machine Learning*, 2020.

[17] Kaiming He, Xiangyu Zhang, Shaoqing Ren, and Jian Sun. Deep residual learning for image recognition. In *Proceedings of the IEEE conference on computer vision and pattern recognition*, pages 770–778, 2016.

[18] Geoffrey Hinton, Oriol Vinyals, and Jeff Dean. Distilling the knowledge in a neural network. *arXiv preprint arXiv:1503.02531*, 2015.

[19] Sanghyun Hong, Varun Chandrasekaran, Yigitcan Kaya, Tudor Dumitras, and Nicolas Papernot. On the effectiveness of mitigating data poisoning attacks with gradient shaping. *CoRR*, abs/2002.11497, 2020.

[20] Sergey Ioffe and Christian Szegedy. Batch normalization: Accelerating deep network training by reducing internal covariate shift. In *International conference on machine learning*, pages 448–456. PMLR, 2015.

[21] Alexander B. Jung, Kentaro Wada, Jon Crall, Satoshi Tanaka, Jake Graving, Christoph Reinders, Sarthak Yadav, Joy Banerjee, Gábor Vecsei, Adam Kraft, Zheng Rui, Jirka Borovec, Christian Vallentin, Semen Zhydenko, Kilian Pfeiffer, Ben Cook, Ismael Fernández, François-Michel De Rainville, Chi-Hung Weng, Abner Ayala-Acevedo, Raphael Meudec, Matias Laporte, et al. imgaug. `https://github.com/aleju/imgaug`, 2020. Online; accessed 01-Feb-2020.

[22] Günter Klambauer, Thomas Unterthiner, Andreas Mayr, and Sepp Hochreiter. Self-normalizing neural networks. *Advances in neural information processing systems*, 30, 2017.

[23] Alex Krizhevsky et al. Learning multiple layers of features from tiny images. 2009.

[24] Ya Le and Xuan Yang. Tiny imagenet visual recognition challenge. *CS 231N*, 7(7):3, 2015.

[25] Yige Li, Xixiang Lyu, Nodens Koren, Lingjuan Lyu, Bo Li, and Xingjun Ma. Neural attention distillation: Erasing backdoor triggers from deep neural networks. In *International Conference on Learning Representations*, 2020.

[26] Yiming Li, Yong Jiang, Zhifeng Li, and Shu-Tao Xia. Backdoor learning: A survey. *IEEE Transactions on Neural Networks and Learning Systems*, 2022.

[27] Yiming Li, Tongqing Zhai, Baoyuan Wu, Yong Jiang, Zhifeng Li, and Shutao Xia. Rethinking the trigger of backdoor attack. *ICLR Workshop on Robust and Reliable Machine Learning in the Real World*, 2021.

[28] Yuezun Li, Yiming Li, Baoyuan Wu, Longkang Li, Ran He, and Siwei Lyu. Invisible backdoor attack with sample-specific triggers. In *Proceedings of the IEEE/CVF International Conference on Computer Vision*, pages 16463–16472, 2021.

[29] Kang Liu, Brendan Dolan-Gavitt, and Siddharth Garg. Fine-pruning: Defending against backdooring attacks on deep neural networks. In *International Symposium on Research in Attacks, Intrusions, and Defenses*, pages 273–294. Springer, 2018.

[30] Yingqi Liu, Wen-Chuan Lee, Guanhong Tao, Shiqing Ma, Yousra Aafer, and Xiangyu Zhang. Abs: Scanning neural networks for back-doors by artificial brain stimulation. In *Proceedings of the 2019 ACM SIGSAC Conference on Computer and Communications Security*, pages 1265–1282, 2019.

[31] Yingqi Liu, Shiqing Ma, Yousra Aafer, Wen-Chuan Lee, Juan Zhai, Weihang Wang, and Xiangyu Zhang. Trojaning attack on neural networks. In *25th Annual Network and Distributed System Security Symposium, NDSS 2018, San Diego, California, USA, February 18-21, 2018*. The Internet Society, 2018.

[32] Yunfei Liu, Xingjun Ma, James Bailey, and Feng Lu. Reflection backdoor: A natural backdoor attack on deep neural networks. In *European Conference on Computer Vision*, pages 182–199. Springer, 2020.

[33] Yuntao Liu, Yang Xie, and Ankur Srivastava. Neural trojans. In *2017 IEEE International Conference on Computer Design (ICCD)*, pages 45–48. IEEE, 2017.

[34] Tuan Anh Nguyen and Anh Tran. Input-aware dynamic backdoor attack. *Advances in Neural Information Processing Systems*, 33:3454–3464, 2020.

[35] Tuan Anh Nguyen and Anh Tuan Tran. Wanet-imperceptible warping-based backdoor attack. In *International Conference on Learning Representations*, 2020.

[36] Han Qiu, Yi Zeng, Shangwei Guo, Tianwei Zhang, Meikang Qiu, and Bhavani Thuraisingham. Deepsweep: An evaluation framework for mitigating dnn backdoor attacks using data augmentation. In *Proceedings of the 2021 ACM Asia Conference on Computer and Communications Security*, ASIA CCS '21, page 363–377, New York, NY, USA, 2021. Association for Computing Machinery.

[37] Adnan Siraj Rakin, Zhezhi He, and Deliang Fan. Tbt: Targeted neural network attack with bit trojan. In *Proceedings of the IEEE/CVF Conference on Computer Vision and Pattern Recognition*, pages 13198–13207, 2020.

[38] Claude Elwood Shannon. A mathematical theory of communication. *The Bell system technical journal*, 27(3):379–423, 1948.

[39] Guangyu Shen, Yingqi Liu, Guanhong Tao, Shengwei An, Qiuling Xu, Siyuan Cheng, Shiqing Ma, and Xiangyu Zhang. Backdoor scanning for deep neural networks through k-arm optimization. In *International Conference on Machine Learning*, pages 9525–9536. PMLR, 2021.

[40] Brandon Tran, Jerry Li, and Aleksander Mądry. Spectral signatures in backdoor attacks. In *Proceedings of the 32nd International Conference on Neural Information Processing Systems*, pages 8011–8021, 2018.

[41] Alexander Turner, Dimitris Tsipras, and Aleksander Madry. Label-consistent backdoor attacks. *arXiv preprint arXiv:1912.02771*, 2019.

[42] Bolun Wang, Yuanshun Yao, Shawn Shan, Huiying Li, Bimal Viswanath, Haitao Zheng, and Ben Y Zhao. Neural cleanse: Identifying and mitigating backdoor attacks in neural networks. In *2019 IEEE Symposium on Security and Privacy (SP)*, pages 707–723. IEEE, 2019.

[43] Dongxian Wu and Yisen Wang. Adversarial neuron pruning purifies backdoored deep models. *Advances in Neural Information Processing Systems*, 34, 2021.

[44] Pengfei Xia, Hongjing Niu, Ziqiang Li, and Bin Li. Enhancing backdoor attacks with multi-level mmd regularization. *IEEE Transactions on Dependable and Secure Computing*, pages 1–1, 2022.

[45] M. Xue, C. He, J. Wang, and W. Liu. One-to-n n-to-one: Two advanced backdoor attacks against deep learning models. *IEEE Transactions on Dependable and Secure Computing*, (01):1–1, oct 5555.

[46] Sangdoo Yun, Dongyoon Han, Seong Joon Oh, Sanghyuk Chun, Junsuk Choe, and Youngjoon Yoo. Cutmix: Regularization strategy to train strong classifiers with localizable features. In *Proceedings of the IEEE/CVF International Conference on Computer Vision*, pages 6023–6032, 2019.

[47] Pu Zhao, Pin-Yu Chen, Payel Das, Karthikeyan Natesan Ramamurthy, and Xue Lin. Bridging mode connectivity in loss landscapes and adversarial robustness. In *International Conference on Learning Representations (ICLR 2020)*, 2020.

Checklist

The checklist follows the references. Please read the checklist guidelines carefully for information on how to answer these questions. For each question, change the default **[TODO]** to [Yes] , [No] , or [N/A] . You are strongly encouraged to include a **justification to your answer**, either by referencing the appropriate section of your paper or providing a brief inline description. For example:

- Did you include the license to the code and datasets? [Yes]
- Did you include the license to the code and datasets? [No] The code and the data are proprietary.
- Did you include the license to the code and datasets? [N/A]

Please do not modify the questions and only use the provided macros for your answers. Note that the Checklist section does not count towards the page limit. In your paper, please delete this instructions block and only keep the Checklist section heading above along with the questions/answers below.

1. For all authors...
   (a) Do the main claims made in the abstract and introduction accurately reflect the paper's contributions and scope? [Yes] See abstract.
   (b) Did you describe the limitations of your work? [Yes] See 5.3
   (c) Did you discuss any potential negative societal impacts of your work? [N/A] There is no negative social impacts of our work.
   (d) Have you read the ethics review guidelines and ensured that your paper conforms to them? [Yes]
2. If you are including theoretical results...
   (a) Did you state the full set of assumptions of all theoretical results? [Yes]
   (b) Did you include complete proofs of all theoretical results? [Yes]
3. If you ran experiments...
   (a) Did you include the code, data, and instructions needed to reproduce the main experimental results (either in the supplemental material or as a URL)? [Yes]
   (b) Did you specify all the training details (e.g., data splits, hyperparameters, how they were chosen)? [Yes] See experimental settings.
   (c) Did you report error bars (e.g., with respect to the random seed after running experiments multiple times)? [Yes] See experimental results.
   (d) Did you include the total amount of compute and the type of resources used (e.g., type of GPUs, internal cluster, or cloud provider)? [Yes] See experimental settings.
4. If you are using existing assets (e.g., code, data, models) or curating/releasing new assets...
   (a) If your work uses existing assets, did you cite the creators? [Yes]
   (b) Did you mention the license of the assets? [Yes]
   (c) Did you include any new assets either in the supplemental material or as a URL? [Yes]
   (d) Did you discuss whether and how consent was obtained from people whose data you're using/curating? [Yes]
   (e) Did you discuss whether the data you are using/curating contains personally identifiable information or offensive content? [N/A]
5. If you used crowdsourcing or conducted research with human subjects...
   (a) Did you include the full text of instructions given to participants and screenshots, if applicable? [N/A]
   (b) Did you describe any potential participant risks, with links to Institutional Review Board (IRB) approvals, if applicable? [N/A]
   (c) Did you include the estimated hourly wage paid to participants and the total amount spent on participant compensation? [N/A]

A Implementation Details of Performed Backdoor Attacks and Defenses

In this part, we provide more detailed information about the state-of-art attacks and defenses applied in our work. The examples of poisoned images are shown in Appendix A.

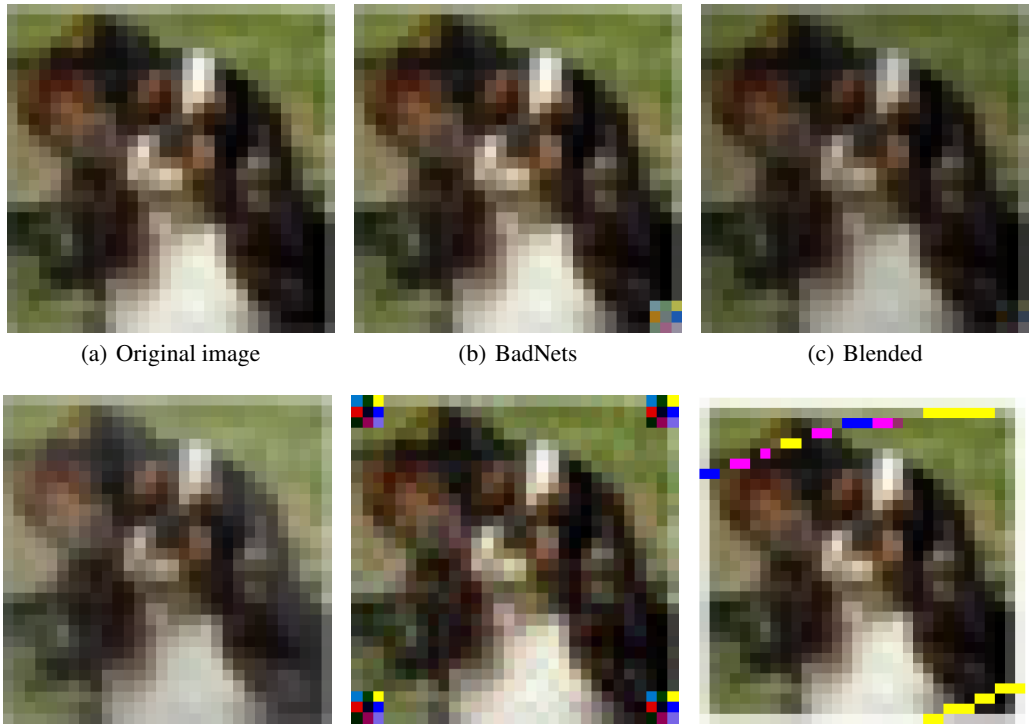

(a) Original image (b) BadNets (c) Blended

(d) Refool (e) CLA (f) IAB

Figure 5: Examples of the poisoned data on CIFAR-10.

(a) Original image (b) SSBA (c) Wa-Net

Figure 6: Examples of the poisoned data on Tiny-ImageNet

The hyperparameter we used in our EP and BNP is 3 in CIFAR-10 and 4 in Tiny-ImageNet. The parameters in other defenses is set as default.

B Additional Experimental Results of Different Poisoning Rate

Poisoning rate is considered important in the proposed methods, since smaller poisoning rate will make the mixture distributions less distinguishable from unimodal distributions. In EP, decreasing poisoning rate will increase the entropy of the backdoor neurons, and it will be harder to precisely

detect them. In BNP, the smaller poisoning rate makes the BN statistics closer to the true benign statistics. Hence, it is important to study the influence of poisoning rate on the performance of the proposed methods. We set the poisoning rate to 1%, 5% and 10% for all attacks and show the results in Table 4. Note that CLA fails to attack the model when the poisoning rate is set to 1%. In most cases, their performances retain a high level. Nevertheless, there are severe degradation against CLA and Refool. Specifically, the ASR of CLA and Refool remain over 10% after pruning using EP and BNP. However, we use default hyperparameter, i.e., $u_h = 3$ and $u_K = 3$ here. By further decreasing the pruning threshold, we can reduce both ASR to less than 5%. Overall, BNP is more robust against attacks of small poisoning rate.

Table 4: Experimental results of the proposed approaches against different attacks compared with other defense methods in CIFAR-10[23].

		BadNets (A2O)		BadNets (A2A)		CLA		WaNet		Blended		Refool		IAB	
ρ	Stage	ACC	ASR	ACC	ASR	ACC	ASR	ACC	ASR	ACC	ASR	ACC	ASR	ACC	ASR
1%	Origin	95.03	99.94	94.75	88.57	88.96	4.73	94.76	46.82	94.17	99.62	93.08	99.59	93.22	64.00
	EP	94.82	0.91	94.17	0.73	87.96	0.65	93.67	14.17	94.46	2.29	91.77	24.08	92.73	5.21
	BNP	92.22	2.16	93.16	7.99	88.03	0.84	94.64	1.24	92.89	2.44	90.99	21.22	93.17	4.19
5%	Origin	94.29	99.99	94.26	92.78	95.53	92.23	94.00	94.55	94.53	81.33	94.35	97.98	92.70	65.50
	EP	93.83	0.83	93.67	0.70	94.43	15.91	92.73	10.13	94.44	5.49	92.75	4.51	92.29	1.83
	BNP	93.61	0.67	93.99	5.64	94.65	12.06	94.17	1.78	93.37	9.21	92.30	2.08	92.74	2.14
10%	Origin	93.89	100.00	94.60	93.89	94.99	98.83	94.11	99.67	94.17	99.63	94.24	98.40	93.87	97.91
	EP	93.88	0.86	94.49	0.61	94.42	0.91	93.79	2.80	93.67	2.24	93.35	8.90	93.17	0.94
	BNP	93.60	1.60	94.25	0.72	94.14	7.03	94.05	3.39	94.17	2.71	93.69	6.48	93.15	0.64

C Additional Experimental Results on Wide-ResNet

To study the generalization of the proposed defense methods over different architectures, we conduct experiments on WideResNet-28-1, which is also a commonly used model in backdoor community. The results are shown in Appendix C.

	Backdoored		EP		BNP	
Attacks	ACC	ASR	ACC	ASR	ACC	ASR
BadNets (A2O)	91.62	99.99	90.30	1.71	91.37	1.61
BadNets (A2A)	92.53	92.03	91.50	0.90	91.43	1.56
CLA	92.81	80.14	91.55	10.24	91.91	4.30
Refool	91.53	97.28	91.11	0.74	90.29	2.87
WaNet	91.78	91.92	92.28	0.67	91.84	0.56
Blended	91.65	99.78	91.59	6.40	91.59	1.52
IAB	90.32	88.08	90.97	1.87	90.74	1.86

D Analysis of Correlation Between Backdoor Neurons and Pruned Neurons

In section Section 3.3, we have demonstrated the definition of sensitivity of neurons to backdoor in Equation (2), which is the difference of backdoor loss before and after being pruned. It is important to ensure that our methods precisely detect those backdoor neurons with high sensitivity. Here, we make scatter plots of the backdoor sensitivity of the neurons and their differential entropy and KL divergence in some typical layers. The detailed scatter figures are shown in Figure 7. The results indicate that both EP and BNP choose the neurons with high sensitivity. Especially for BadNets, the highest sensitivity of one single neuron is extremely large and its differential entropy and KL divergence stay away from average. The overall results demonstrate a strong correlation between the neuron sensitivity to backdoor and the proposed indices.

E Performance on Low-quality Data

Our methods require extra data and rely on its distribution to detoxify the backdoor model, so it's natural to consider a worse case that we can only get low-quality dataset with some distortion in it. To further show the effectiveness of our proposed methods, we utilize multiple data augmentation tricks

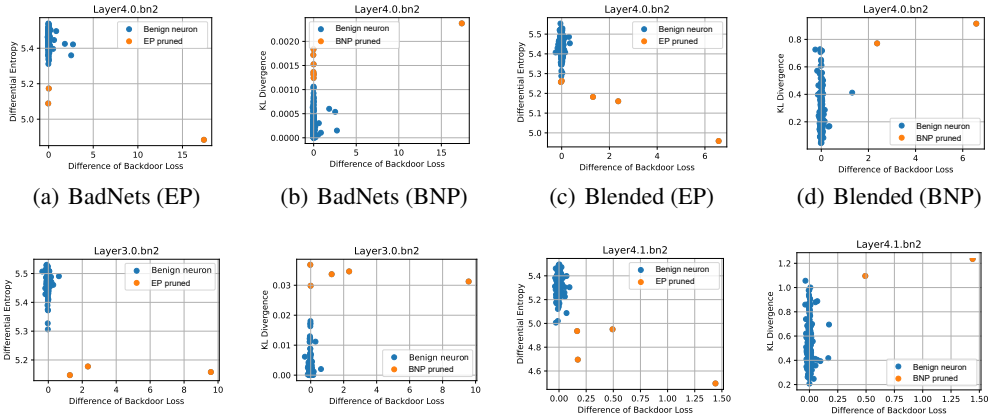

(a) BadNets (EP) (b) BadNets (BNP) (c) Blended (EP) (d) Blended (BNP)

(e) WaNet (EP) (f) WaNet (BNP) (g) Refool (EP) (h) Refool (BNP)

Figure 7: Scatter plots of backdoor sensitivity of mid-layer neurons to backdoor and the corresponding differential entropy and KL divergence indices.

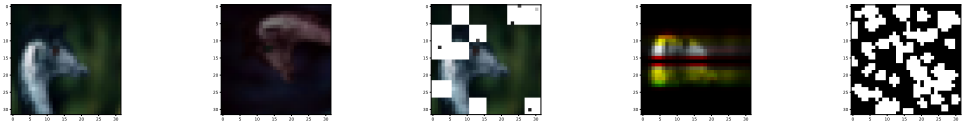

(a) Original image (b) CJ (c) SAP (d) PW (e) Snow

Figure 8: Examples of the perturbed data.

to create out-of-distribution data on CIFAR-10 while performing defenses against BadNets (A2O) attack, including color jitter with 90 degree rotation (CJ) from torchvision, CoarseSaltandPepper (SAP), PolarWarping (PW), Snowflakes (Snow) from [21]. To be specific, the parameters of CJ are set to be [0.5, 0.5, 0.5, 0.5]; 30% of the pixels in SAP are replaced replaced by salt/pepper noise mask which has 1% to 10% the size of the input image; the translate percent in PW is set to be ± 0.2; the snow size of Snow is (0.2, 0.5) and its speed is (0.01, 0.05). Samples of those perturbed images are shown in Appendix E. Now we replace 10% of the EP and BNP used data into those perturbed out-of-distribution data, and see the performance of our methods. The experimental results are shown in Table 5, which illustrates that even if some low-quality data are mixed into the data they use, our methods can still successfully locate the backdoor neurons and delete them while maintaining high clean accuracy.

Table 5: Experimental Results of the proposed methods using low-quality datasets.

	Origin		CJ		SAP		PW		Snow	
Attacks	ACC	ASR	ACC	ASR	ACC	ASR	ACC	ASR	ACC	ASR
EP	93.88	0.86	93.62	0.88	93.19	0.86	93.65	0.82	93.23	0.93
BNP	93.60	1.60	93.56	1.52	91.17	1.58	92.62	0.96	90.99	0.95

F Detailed Comparison on Neuron Pruing Accuracy

To evaluate the accuracy in locating malicious neurons of the proposed methods and the SOTA pruning-based method ANP, we record the minimum pruning amount that can lead to acceptable degradation on ASR. Specifically, we gradually change the hyperparameter u of EP, BNP and the pruning threshold of ANP until their ASRs drop below 10%, which we regard as a sign of successful defense. The detailed results are shown in Table 6.

Table 6: The number of pruned neurons for EP, BNP and ANP to be able to achieve considerable defending performance.

	EP			BNP			ANP		
Attacks	ACC	ASR	#Pruned	ACC	ASR	#Pruned	ACC	ASR	#Pruned
BadNets(A2O)	93.86	5.22	2	93.84	1.84	3	93.6	5.23	4
BadNets(A2A)	94.73	2	7	94.64	7.7	10	80	3.44	235
Blended	94.21	3.4	2	94.21	3.4	2	93.84	5.21	27
CLA	94.86	7.11	19	94.07	9.67	71	91.45	7.2	256
Refool	93.18	8.94	79	93.97	7.12	6	63.91	1.29	186
IAB	93.67	8.07	10	93.68	7.63	6	93.27	4.83	36
WaNet	93.43	4.06	43	94.87	9.64	13	94.99	1.31	3
SSBA(TinyImageNet)	66.41	4.13	5	66.36	6.04	5	66.49	2.81	7

Under most situations, our proposed EP and BNP show higher or similar pruning precision in finding malicious neurons than ANP. Moreover, our pruning methods gives promising pruning results when u_k/u_h is around 3 as we suggested, since most of the pruning has achieved considerable results before u_k/u_h reaches 3. You can refer to Appendix D for detailed pruning performance. However, for ANP, it is hard to choose a proper mask value threshold of the neurons to be pruned, and it is also not practical to select a specific number of neurons to finish the pruning. Moreover, the higher the mask value of neurons, the more dense the neurons are, making it harder to find a suitable value for pruning threshold, since there will be huge difference on ACC and ASR with slight change of threshold. In summary, our proposed EP and BNP can locate the neurons more precisely in most situations, and gives an easier way to prune the malicious neurons.

G Exploration of Potential Adaptive Attacks

In this section, we explore some potential adaptive attacks against the proposed methods.

G.1 BN Re-parameterization against BNP

The BNP pruning strategy rely on the correct information from the BN statistics. However, this information can be changed by a defense-aware attacker using re-parameterization techniques. Specifically, consider a BN operation performed on each neuron by:

$$\begin{aligned}\tilde{\mathrm{BN}}^{(l)}(\boldsymbol{x}_k^{(l)})_{\tilde{\gamma}_k^{(l)},\tilde{\beta}_k^{(l)}} &= \tilde{\gamma}_k^{(l)}\frac{\boldsymbol{x}_k^{(l)}-\tilde{\mu}_k^{(l)}}{\tilde{\sigma}_k^{(l)}}+\tilde{\beta}_k^{(l)} \\ &= \frac{\tilde{\gamma}_k^{(l)}}{\tilde{\sigma}_k^{(l)}}\boldsymbol{x}_k^{(l)}+(\tilde{\beta}_k^{(l)}-\frac{\tilde{\mu}_k^{(l)}}{\tilde{\sigma}_k^{(l)}}).\end{aligned}$$

The attacker can calculate the sample statistics denoting $\mu_k^{(l)}$ and $\sigma_k^{(l)}$ from benign data, and assign new weights and bias by:

$$\begin{aligned}\gamma_k^{(l)} &= \frac{\sigma_k^{(l)}}{\tilde{\sigma}_k^{(l)}}\tilde{\gamma}_k^{(l)} \\ \beta_k^{(l)} &= \tilde{\beta}_k^{(l)}-\frac{\tilde{\mu}_k^{(l)}}{\tilde{\sigma}_k^{(l)}}+\frac{\mu_k^{(l)}}{\sigma_k^{(l)}}\end{aligned}$$

In this way, the whole linear transformation remains unchanged, but the BN statistics become consistent with that of the benign data, which makes the backdoor neurons unable to be detected by the proposed BNP.

G.2 Regularization-based Adaptive Attacks

Both of the two methods rely on the discrepancy of the benign distribution and poisoned distribution. Hence, we wonder whether EP and BNP still work if the attacker try to regularize the distribution to

Table 7: Experimental results on regularization-based adaptive attack.

	$\lambda = 1$		$\lambda = 0.1$		$\lambda = 0.01$		$\lambda = 0.001$	
Attacks	ACC	ASR	ACC	ASR	ACC	ASR	ACC	ASR
Origin	NaN	NaN	NaN	NaN	95.11	100.00	93.41	75.30
EP	—	—	—	—	93.63	9.23	93.35	0.63
BNP	—	—	—	—	94.15	0.32	93.82	0.24

Table 8: Experimental results of our methods against some existing adaptive attacks.

	ML-MMD		WB	
	ACC	ASR	ACC	ASR
Origin	87.51	98.48	92.12	100
EP	86.34	3.26	90.88	24.65
BNP	86.9	36.15	90.88	37.4

minimize the discrepancy. Hence, we use BadNets as an example to perform the adaptive attack with an additional objective:

$$\mathcal{L}_{adaptive} = \mathbb{E}_{(\boldsymbol{x},y)\sim\mathcal{D}}[\mathrm{D}_{\mathrm{CE}}(y, f(\delta(\boldsymbol{x}))] + \lambda \sum_{1\leq k\leq K} \sum_{1\leq l\leq L} \mathbb{E}_{\boldsymbol{x}\sim\mathcal{X}}[(\boldsymbol{\phi}_k^{(l)} - \hat{\boldsymbol{\phi}}_k^{(l)})^2], \tag{4}$$

where $\boldsymbol{\phi}_k^{(l)}$ and $\hat{\boldsymbol{\phi}}_k^{(l)}$ denote the pre-activations of benign and poisoned samples in the kth neuron of the lth layer. The goal of the second term is to minimize the discrepancy between the benign distribution and the poisoned distribution with a trade-off hyperparameter λ. We select λ from [1.000, 0.100, 0.010, 0.001] and train four models and do pruning using EP and BNP, the results are shown in Table 7. We find that too large λ makes the objective not trainable, hence collapse the training process. This may because it is not realistic to distinguish benign and poisoned samples while making their distribution indistinguishable. After down weighting λ, the model is able to be trained normally. However, we find EP and BNP are still able to remove the backdoor without influence too much on the clean accuracy.

A recently proposed method[44] also regularizes the distribution discrepancy between benign samples and poisoned samples by Multi-Level Maximum Mean Discrepancy (ML-MMD), which is a direct attack against our defense. Besides, [11] propose to use wasserstein distance to minimize the difference between poison and clean data latent feature distribution (WB). We test our methods on them and find they still work with some degradation. The results are shown in Table 8. The main reason for such degradation is the strong constraint added to minimize the difference between clean and poison data latent feature distribution. Besides, both the above attacks adds constraint to loss function, making it harder to converge during training process, and their final ACC is obviously lower than normal attacks.

H Additional Experimental Results for the Choice of Hyperparameter

In this section, we provide ablation study on the choice of the threshold hyperparameter u_h/u_k. As shown in Figure 9, both EP and BNP gives promising defending results against most tested attacks on CIFAR 10 when u_h/u_k is around 3.Besides, the robustness of the hyperparameter is supported by the wide choice of available u_h/u_k that lead to acceptable results.

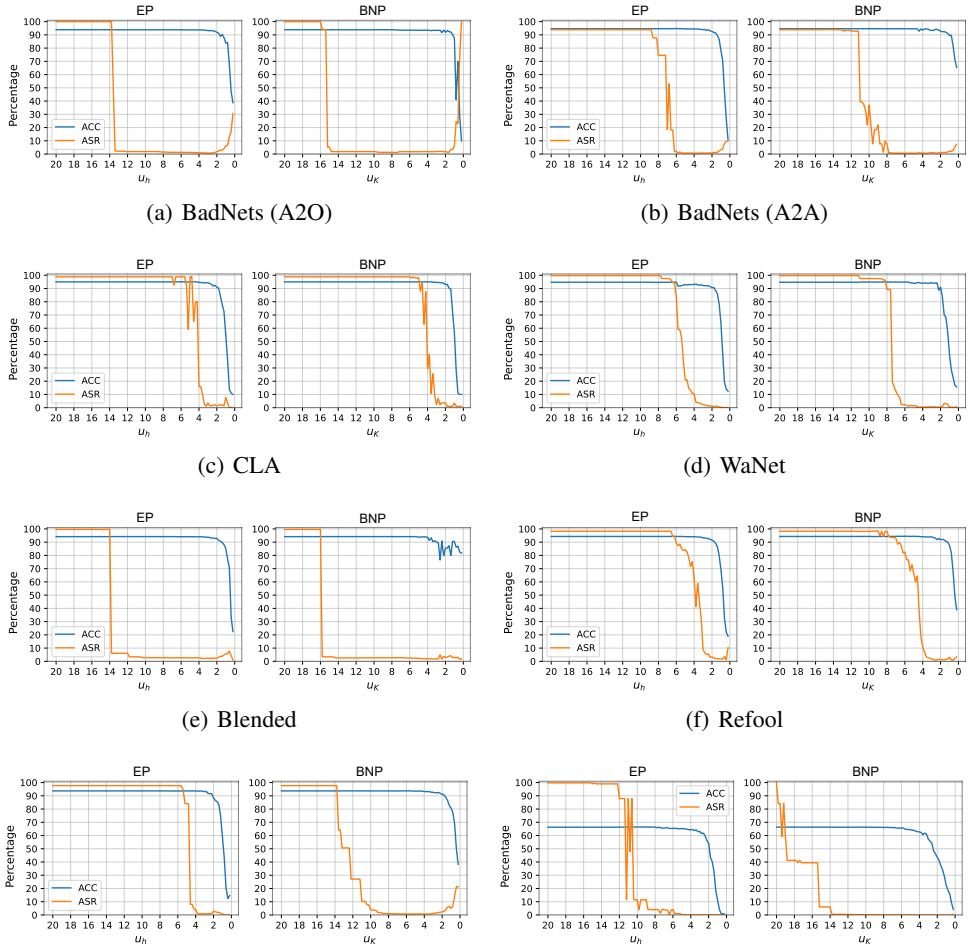

(a) BadNets (A2O)

(b) BadNets (A2A)

(c) CLA

(d) WaNet

(e) Blended

(f) Refool

(g) IAB

(h) SSBA (TinyImageNet)

Figure 9: The performance of proposed EP and BNP with different hyperparameter u_h/u_k against all the tested attacks on ResNet-18.